Proc. Natl. Acad. Sci. USA
Vol. 96, pp. 9142–9147, August 1999
Developmental Biology

A vital role for glycosphingolipid synthesis during development and differentiation

TADASHI YAMASHITA*, RYUICHI WADA*, TEIJI SASAKI*, CHUXIA DENG*, UWE BIERFREUND†, KONRAD SANDHOFF†, AND RICHARD L. PROIA*‡

*Genetics of Development and Disease Branch, National Institute of Diabetes and Digestive and Kidney Diseases, National Institutes of Health, Bethesda, MD 20892; and †Kekulé-Institut für Organische Chemie und Biochemie der Universität Bonn, Gerhard-Domagk-Strasse 1, 53121, Bonn, Germany

Edited by Stuart A. Korneld, Washington University School of Medicine, St. Louis, MO, and approved June 3, 1999 (received for review March 3, 1999)

ABSTRACT **Glycosphingolipids (GSLs) are believed to be integral for the dynamics of many cell membrane events, including cellular interactions, signaling, and trafficking. We have investigated their roles in development and differentiation by eliminating the major synthesis pathway of GSLs through targeted disruption of the *Ugcg* gene encoding glucosylceramide synthase. In the absence of GSL synthesis, embryogenesis proceeded well into gastrulation with differentiation into primitive germ layers and patterning of the embryo but was abruptly halted by a major apoptotic process. *In vivo*, embryonic stem cells deficient in GSL synthesis were again able to differentiate into endodermal, mesodermal, and ectodermal derivatives but were strikingly deficient in their ability to form well differentiated tissues. *In vitro*, however, hematopoietic and neuronal differentiation could be induced. The results demonstrate that the synthesis of GSL structures is essential for embryonic development and for the differentiation of some tissues and support the concept that GSLs are involved in crucial cell interactions mediating these processes.**

Glycosphingolipids (GSLs) are present on virtually all mammalian cell plasma membranes§ (2). They are amphipathic molecules consisting of a ceramide lipid moiety, embedded in the outer leaflet of the membrane, linked to one of hundreds of different externally oriented oligosaccharide structures. A subclass of GSLs that contain sialic acid residues are known as gangliosides and have special prominence in the nervous system. GSLs have been implicated in many fundamental cellular processes, including growth, differentiation, migration, and morphogenesis; cell-to-cell and cell-to-matrix interactions; and the development and functioning of the nervous system (3–10).

GSLs are believed to be integral components of plasma membrane microdomains, known as rafts and caveolae (11–14), that are rich in sphingolipids and cholesterol. These lipid domains assemble receptors and glycosylphosphatidylinositol-anchored proteins on their external surface and signaling molecules—Src-family kinases, G proteins, nitric oxide synthase—on their inner surface and mediate membrane trafficking and signal activity. A second type of GSL domain consisting primarily of GSLs and signal transduction molecules has been proposed to couple cell adhesion interactions with signaling (15, 16).

The core structure of the majority of GSLs, glucosylceramide, is synthesized on the cytoplasmic face of the Golgi by glucosylceramide synthase via the transfer of a glucose residue from UDP-glucose to ceramide (17, 18). Glucosylceramide synthase is a transmembrane protein with its C-terminal catalytic domain located in the cytoplasm (19). After glucosylceramide is synthesized and translocated into the Golgi lumen, it is modified by a series of Golgi glycosyltransferases to produce higher-order GSL structures. To enable a direct determination of the function and biological roles of GSLs arising from glucosylceramide, we have disrupted the gene (*Ugcg*) encoding glucosylceramide synthase to eliminate the major pathway of GSL synthesis (Fig. 1*A*). Our results demonstrate that GSL synthesis is vital for embryonic development and also for the differentiation of certain tissues.

MATERIALS AND METHODS

Targeting Constructs, Gene Targeting, and Generation of Mutant Mice. One genomic clone containing the *Ugcg* locus was isolated from a 129-mouse library (Genome Systems; St Louis) by using a mouse *Ugcg* cDNA probe. A 5-kilobase (kb) *Pst*I fragment containing exon 5 and exon 6 and a 4.5-kb *Xba*I fragment containing exon 8, exon 9, and the 3′ untranslated region were used together with neomycin (20), hygromycin (21), and thymidine kinase (20) expression cassettes to construct targeting vectors *pUgcgNeo* (Fig. 1*B*) and *pUgcgHygro* (Fig. 1*C*). *Not*I was used to linerize each of the vectors for gene targeting.

Culture and targeting of TC-1 embryonic stem (ES) cells and establishment of chimeric mice were performed as in past experiments (22, 23). Second-round gene targeting and hygromycin selection to establish ES cells with a deletion in both *Ugcg* alleles was accomplished as described (24).

Histology, Immunostaining, Apoptotic Analysis, and *in Situ* Hybridization of Embryos. Embryonic day (E) 6.5 and 7.5 embryos were removed together with decidual tissue. They were fixed in 10% buffered formalin and were processed for paraffin embedding. Sections 4 μm thick were stained with hematoxylin and eosin (H & E), and were immunostained. Immunostaining of proliferating cell nuclear antigen (PCNA) was performed with PCNA Staining Kit (Zymed).

Apoptotic cell death was detected by the *in situ* DNA nick end-labeling [terminal deoxynucleotidyltransferase-mediated UTP end labeling (TUNEL)] method using an Apoptag kit (Oncor). *In situ* hybridization was accomplished with digoxigenin-labeled *Brachyury* (25), *Cerr1* (26), *HNF3β* (27), *Otx2* (28), and *H19* (29) probes and an antidigoxigenin antibody-alkaline phosphatase conjugate (Boehringer Mannheim) as described (30).

Genotype Analysis of Embryos. For DNA recovery, embryonic tissue was scrapped from paraffin sections and was incubated with 10 μl of lysis solution (0.6 mg/ml proteinase K/10 mM Tris·HCl/50 mM KCl/2.5 mM $MgCl_2$/0.1% gelatin/0.45% Non-

The publication costs of this article were defrayed in part by page charge payment. This article must therefore be hereby marked "*advertisement*" in accordance with 18 U.S.C. §1734 solely to indicate this fact.

PNAS is available online at www.pnas.org.

This paper was submitted directly (Track II) to the *Proceedings* office.
Abbreviations: E, embryonic day; ES cells, embryonic stem cells; GSL, glycosphingolipid; kb, kilobase; H & E, hematoxylin and eosin; PCNA, proliferating cell nuclear antigen; TUNEL, terminal deoxynucleotidyltransferase-mediated UTP end labeling; HPTLC, high-performance thin-layer chromatography; C6-NBD-ceramide, 6-((*N*-(7-nitrobenz-2-oxa-1,3-diazol-4-yl)amino)hexanoyl)sphingosine.

‡To whom reprint requests should be addressed at Building 10, Room 9D-20, 10 Center Drive, MSC 1810, National Institutes of Health, Bethesda, MD 20892. E-mail: proia@nih.gov.

§Ganglioside nomenclature used in this paper is that of Svennerholm (1).

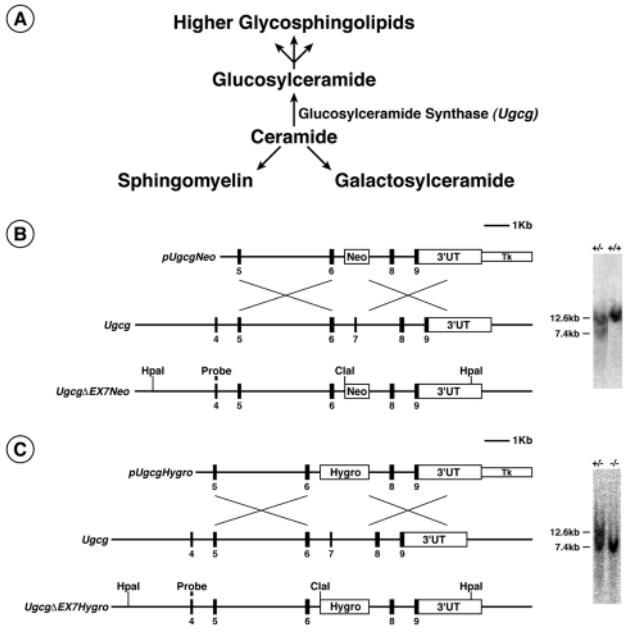

FIG. 1. *Ugcg* gene targeting. (*A*) The biosynthetic pathways for sphingolipids. Glucosylceramide is produced by the modification of ceramide by glucosylceramide synthase. Glucosylceramide is the core structure for the synthesis of higher-order GSLs. Ceramide also is used for synthesis of sphingomyelin and galactosylceramide. (*B*) The structure of the *pUgcgNeo* targeting vector is shown at the top. The wild-type *Ugcg* locus is in the middle. The structure of the targeted locus ($Ugcg^{\Delta EX7Neo}$) is on the bottom. The $Ugcg^{\Delta EX7Neo}$ locus was detected by Southern blot analysis of genomic DNA after digestion with *Hpa*I and *Cla*I and hybridization with the probe indicated. The wild-type allele yielded a 12.6-kb fragment, and the $Ugcg^{\Delta EX7Neo}$ allele yielded a 7.4-kb fragment. The Southern blots were from tail DNA of wild-type (+/+), and $Ugcg^{\Delta EX7Neo/+}$ (+/−) mice derived from targeted ES cells. (*C*) The structure of the *pUgcgHygro* targeting vector is shown at the top. The wild-type *Ugcg* locus is in the middle. The structure of the targeted allele, $Ugcg^{EX7Hygro}$, is on the bottom. The $Ugcg^{EX7Hygro}$ locus was detected by Southern blot analysis of genomic DNA after digestion with *Hpa*I and *Cla*I and hybridization with the probe indicated. The wild-type allele yielded a 12.6-kb band, and the $Ugcg^{\Delta EX7Neo}$ and $Ugcg^{\Delta EX7Hygro}$ alleles each yielded a 7.4-kb fragment. The Southern blots were of DNA of $Ugcg^{\Delta EX7Neo}$ (+/−) ES cells and doubly targeted ES cells $Ugcg^{\Delta EX7Neo/\Delta EX7Hygro}$ (−/−).

idet P-40/0.45% Tween 20) at 60°C overnight and then at 99°C for 10 min. Embryos obtained by dissection were treated the same except the volume of lysis buffer was 70 μl.

For genotyping by PCR, the primers were 5′-CAATGGCTGAAGAGCATTCAG-3′ (Primer 1), 5′-AACAGAACAAACTTTTCTGGA-3′ (Primer 2), and 5′-TCGCCTTCTTGACGAGTTCTTCTGAG-3′ (Primer 3). Primers 1 and 2 detected the wild-type *Ugcg* allele and amplified an ≈500-bp fragment. Primers 2 and 3 detected the $Ugcg^{\Delta EX7Neo}$ allele and amplified an ≈200-bp fragment. The PCR reaction volume was 20 μl, including 5 μl of DNA solution.

Glucosylceramide Synthase Enzyme Assay and Lipid Analysis. Glucosylceramide synthase activity was assayed with 6-((*N*-(7-nitrobenz-2-oxa-1,3-diazol-4-yl)amino)hexanoyl)sphingosine (C6-NBD-ceramide) (Molecular Probes) according to the method of Lipsky and Pagano (31). Neutral and acidic lipid fractions from ES cells and teratomas were isolated and analyzed as described (23).

Teratomas. Wild-type ES cells and ES cells with both *Ugcg* alleles disrupted (1×10^6) were injected into subcutaneous sites on syngeneic 129/SvEv mice. After 3 weeks, each tumor was carefully excised, and three cut surfaces were made. Tumors were fixed in 10% buffered formalin and were processed to be embedded in paraffin. Sections 4 μm thick were stained with H & E and Alcian blue. The tumor components were evaluated as to the origin from the three germ cell layers and the degree of differentiation. The elements were classified according to their resemblance to tissues of embryo and adult mouse tissues. Undifferentiated epithelium that had no similarity to mature tissues was categorized as poorly differentiated epithelium. Eight *Ugcg* mutant tumors were evaluated with similar conclusions. Sections were immunostained with PCNA (Zymed) and vimentin antibodies (Sigma). Apoptotic cells were detected by the TUNEL method as described above.

ES Cell Differentiation *in Vitro*. ES cells were cultured under conditions for the formation of simple embryoid bodies and cystic embryoid bodies essentially as described by Robertson (32). At days 14 and 22 in culture under differentiation conditions, the embryoid bodies were fixed in 10% buffered formalin, were processed, and were embedded in paraffin. Sections 4 μm thick were stained with H & E.

Neuronal differentiation of embryoid bodies was induced with retinoic acid as described (24). Neuronal differentiation was judged by neurite formation and immunostaining with GAP43 antibody (Sigma). Erythroid differentiation was accomplished by treatment of embryoid bodies in methylcellulose with erythropoietin (33). Erythroid cell differentiation was established by the appearance of hemoglobinized (red) cells around the embryoid body.

RESULTS

Targeting the *Ugcg* Gene for Disruption. The *Ugcg* gene in TC-1 ES cells (22) was disrupted by using a targeting vector (*pUgcgNeo*) in which Exon 7 of the *Ugcg* gene was deleted (Fig. 1*B*). Homologous recombination of the *Ugcg* locus using the *pUgcgNeo* targeting vector was confirmed by Southern blot analysis and demonstrated that 14 ES cell clones of 85 contained a targeted gene disruption termed $Ugcg^{\Delta EX7Neo}$.

With the $Ugcg^{\Delta EX7Neo}$ mutation, sequences from the cytoplasmically exposed, catalytic domain of glycosylceramide synthase were removed, with the expectation that the enzyme would be inactivated. An ES clone containing the $Ugcg^{\Delta EX7Neo}$ allele was injected into mouse blastocysts for the production of chimeric mice. The clone resulted in germline transmission of the $Ugcg^{\Delta EX7Neo}$ allele.

Disruption of the *Ugcg* Gene Results in Embryonic Lethality. No *Ugcg* homozygous mutant mice were detected among 134 offspring from $Ugcg^{\Delta EX7Neo/+}$ intercrosses (Table 1). The results indicated that the consequence of homozygosity for the mutant *Ugcg* allele was embryonic lethality.

To determine the time of lethality, embryos from $Ugcg^{\Delta EX7Neo/+}$ intercrosses were analyzed at different days postcoitum (Table 1). Genotyping was accomplished by PCR analysis of embryos. At E6.5, $Ugcg^{\Delta EX7Neo}$ homozygous embryos were present and could not be distinguished from wild-type or heterozygous embryos by gross morphology. At E7.5, ≈25% of the embryos were found to be homozygous for the mutation (Table 1), and they could now be distinguished from wild-type and heterozygous embryos by their smaller size. At E8.5, the $Ugcg^{\Delta EX7Neo}$ homozygous embryos consisted of a small remnant

Table 1. Genotype analysis of offspring from *Ugcg* heterozygous intercrosses

Age	Total	Genotype			Empty decidua
		+/+	+/−	−/−	
E6.5	24	7	14	3	0
E7.5	88	17	49	22*	0
E8.5	54	8	31	15†	0
E9.5	101	27	46	0	28
Postnatal	134	48	86	0	

*Abnormally small.
†Remnant.

of embryonic tissue that was apparently in the process of resorption. At E9.5, the resorption of homozygous mutant embryos appeared complete because none of the recovered embryos yielded the $Ugcg^{\Delta EX7Neo/\Delta EX7Neo}$ genotype. Correspondingly, ≈25% of egg cylinders were without embryonic tissue at this stage (Table 1). These results show that disruption of GSL synthesis caused embryonic lethality beginning about E7.5 with complete resorption of the embryo by E9.5.

Embryonic Lethality Occurs at Gastrulation. Analysis of the histology of $Ugcg^{\Delta EX7Neo}$ homozygous embryos was accomplished by examination of serial sections of E6.5 and E7.5 embryos obtained from heterozygous crosses. At E6.5, the sectioned embryos were not distinguishable histologically, by PCNA expression, or by TUNEL assay (data not shown). However, at E7.5, there were profound differences. At this developmental stage, the wild-type and heterozygous embryos were undergoing gastrulation and contained the three germ cell layers: mesoderm, endoderm, and ectoderm (Fig. 2*C*). The three major cavities—exoceolom, amniotic, and ectoplacental—were easily identified (Fig. 2*A*). $Ugcg^{\Delta EX7Neo/\Delta EX7Neo}$ embryos also were undergoing gastrulation, as evidenced by formation of mesoderm as a distinct cell layer between endoderm and ectoderm (Fig. 2*D*) and by expression of the early mesodermal marker, *Brachyury* (T gene) (Fig. 2 *E* and *F)*. The expression of other genes that specify cell lineage differentiation and patterning during gastrulation also appeared relatively normal in the mutant embryos. These included *HNF3β* (27), expressed in visceral and definitive endoderm and node (data not shown), *Cerr1* (26), expressed in anterior endoderm (Fig. 2*H*), and *Otx2* (28), expressed in the anterior germ layers (data not shown).

Morphologic and gene expression criteria indicated that the mutant embryos had proceeded well into the gastrulation stage. However, they exhibited a number of abnormalities when compared with normal embryos. They were smaller in size with a reduced extraembryonic portion relative to the embryonic portion (Fig. 2*B*). This impression was confirmed by *in situ* hybridization with an H19 probe, a marker specific for the extraembryonic cell types (29) (data not shown). The three major embryonic cavities were present but appeared disorganized and significantly reduced in size (Fig. 2*B*). The fact that an exoceolom was present in the $Ugcg^{\Delta EX7Neo}$ homozygous embryos indicated that mesodermal migration into the extraembryonic segment had occurred. Reichert's membrane, a basement membrane produced by the parietal endoderm, appeared to be adhering to the decidua in the $Ugcg^{\Delta EX7Neo}$ homozygous embryos (Fig. 2 *A* and *B*).

We next examined whether the reduced size of the E7.5 $Ugcg^{\Delta EX7Neo}$ homozygous embryos might be caused by an impairment of cellular proliferation or an increase in cell death. Immunohistochemical detection of PCNA revealed that cell proliferation in the mutant embryos was similar or slightly increased compared with wild-type embryos (Fig. 2 *I* and *J*).

TUNEL assay on sections of E7.5 embryos revealed a large increase in cells undergoing apoptosis in the $Ugcg^{\Delta EX7Neo}$ homozygous embryos compared with wild-type and heterozygous embryos (Fig. 2 *K* and *L*). The ectodermal layer was particularly enriched in the TUNEL positive cells. However, increased apoptosis was noted in other regions of the embryo as well.

We conclude that, in the absence of GSL synthesis, embryogenesis proceeded into the gastrulation stage, from which the death of the embryo rapidly ensued. Greatly enhanced apoptosis centered in the ectoderm appeared to be a primary cause of embryonic death.

Differentiation *in Vitro* Without GSL Synthesis. To analyze consequences of the absence of GSL synthesis at a cellular level, we disrupted both *Ugcg* alleles in ES cells. This was accomplished by a second round of gene targeting in *Ugcg* heterozygous ES cells with a *Ugcg* targeting vector containing a hygromycin selectable marker (*pUgcgHygro*; Fig. 1*C*). The targeting vector was configured in a manner similar to *pUgcgNeo* (Fig. 1*B*) and resulted in the deletion of exon 7 of the wild-type *Ugcg* allele after homologous recombination.

Extracts from the $Ugcg^{\Delta EX7Neo/\Delta EX7Hygro}$, $Ugcg^{\Delta EX7Neo/+}$ and wild-type cells were assayed for glucosylceramide synthase activity (Fig. 3*A Inset*). The $Ugcg^{\Delta EX7Neo/+}$ extract contained approximately half the glucosylceramide synthase activity of the wild-type extract whereas the $Ugcg^{\Delta EX7Neo/\Delta EX7Hygro}$ extract was without detectable enzyme activity, proving that a complete elimination of glucosylceramide synthase activity was achieved through the targeted disruption of the *Ugcg* gene. Glucosylceramide and lactosylceramide were detected in neutral lipids in wild-type ES cells but not in the $Ugcg^{\Delta EX7Neo/\Delta EX7Hygro}$ ES cells (Fig. 3*B*) whereas acidic GSLs were detected in neither cell type (data not shown). Levels of sphingomyelin (Fig. 3*B*) and ceramide (Fig. 3*C*) were similar in wild-type and mutant ES cells. Although glucose-based GSL synthesis pathway was absent in $Ugcg^{\Delta EX7Neo/\Delta EX7Hygro}$ cells, their rate of growth was indistinguishable from heterozygous and wild-type ES cells (Fig. 3*A*).

To determine the *in vitro* differentiation capacity of $Ugcg^{\Delta EX7Neo/\Delta EX7Hygro}$ ES cells, undifferentiated wild-type and mutant ES cells were trypsinized, were seeded into bacteriological Petri dishes, and were induced to differentiate by removal of leukemia inhibitory factor and β-mercaptoethanol from the culture media. After 3–4 days in culture, both the wild-type cells and mutant ES cells had aggregated into densely packed clusters to form simple embryoid bodies (Fig. 3 *D* and *E*). After an additional week in culture, both types of embryoid bodies underwent further differentiation to form cystic embryoid bodies (34) (Fig. 3 *F* and *G*). On histologic sections, the outer layer of both types of cystic bodies were made up of endodermal cells with the inner layer composed of neuroectodermal cells, although the mutant cystic bodies contained a greater predominance of immature neuroectodermal tissue (data not shown).

Wild-type and $Ugcg^{\Delta EX7Neo/\Delta EX7Hygro}$ ES cells were induced to differentiate along a neuronal pathway with retinoic acid (24, 35) and along a hematopoietic pathway by treatment with erythropoietin (33). The mutant ES cells, like wild-type cells, differentiated into cells with a neuronal morphology, as evidenced by neurite formation (Fig. 3 *H* and *I*) and GAP43 expression (data not shown). The mutant ES cells were also similar to wild-type cells in their ability to differentiate into erythroid cells in methylcellulose, as indicated by hemoglobination of the colonies (Fig. 3 *J* and *K*).

Differentiation *in Vivo* Without GSL Synthesis. Wild-type and the $Ugcg^{\Delta EX7Neo/\Delta EX7Hygro}$ ES cells were injected into subcutaneous sites of syngeneic 129/SvEv mice to produce teratomas. The size range of tumors derived from the mutant ES cells were similar to sizes of the wild-type tumors. The mutant tumor tissue was largely devoid of acidic lipids, which include gangliosides, in comparison to their abundant expression in the wild-type tumor (Fig. 4*A*). The neutral lipid fraction of the mutant tumor showed a slight increase (35%) in sphingomyelin (Fig. 4*B*). Ceramide levels in the wild-type and mutant tumor tissue were similar (Fig. 4*C*).

Histological examination revealed critical differences between the wild-type and mutant tumors in the types of cells and tissues present. The major component in both types of tumors was neuronal tissue, primarily composed of glial cells enmeshed in loose connective tissue. This component made up a far greater percentage of the mutant tumors than the wild-type tumors. The remainder of the tissues in the mutant tumors consisted primarily of primitive neuroectoderm and poorly differentiated and disorganized epithelial tissues (Fig. 4*G*).

In contrast to the preponderance of the undifferentiated tissue in the mutant tumors, the wild-type tumors contained easily identified mature tissues. Positive Alcian blue staining, indicative of cartilage and bone tissue, was clearly discernible in the wild-type but virtually absent from the mutant tumors (Fig. 4 *D* and *E*). Smooth muscle and cartilage were apparent in the

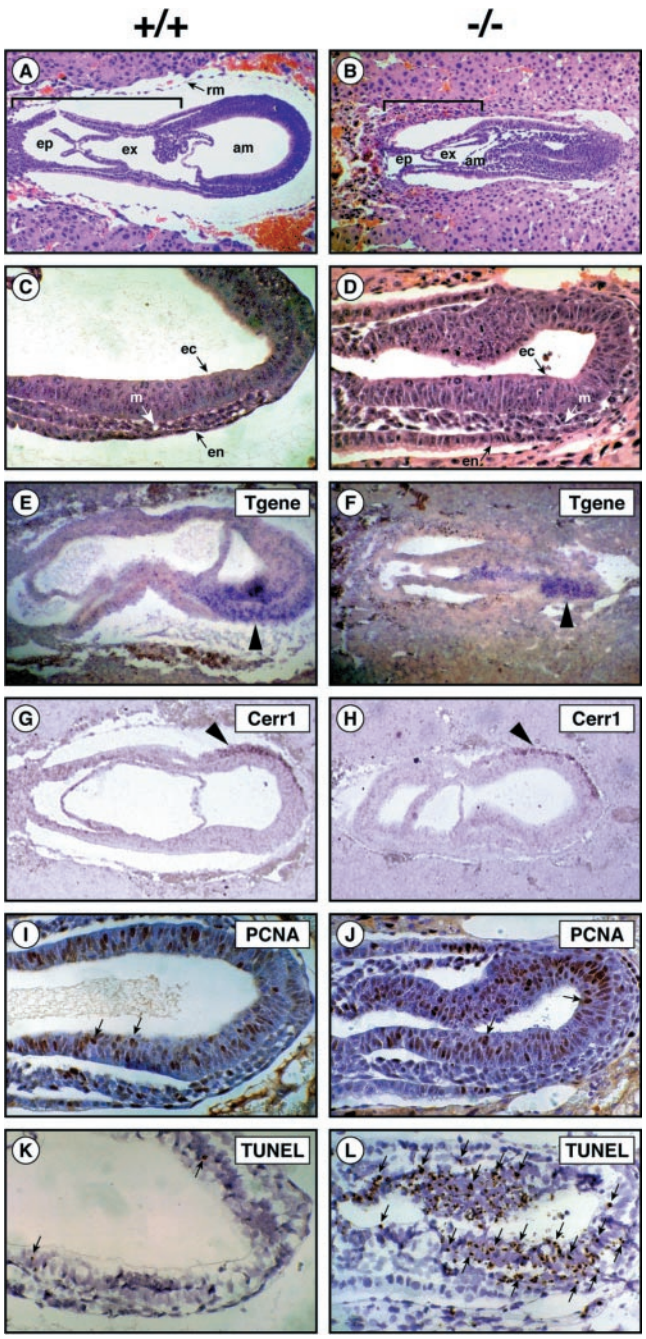

FIG. 2. Histology of mutant *Ugcg* embryos. E7.5 embryos were obtained from timed matings between $Ugcg^{\Delta EX7Neo/+}$ males and $Ugcg^{\Delta EX7Neo/+}$ females. *A*, *C*, *E*, *G*, *I*, and *K* show wild-type embryos (+/+). *B*, *D*, *F*, *H*, *J*, and *L* show $Ugcg^{\Delta EX7Neo/\Delta EX7Neo}$ embryos (−/−). (*A* and *B*) Comparison of the organization of embryos by H & E staining of paraffin sections. The cavities are indicated. Note the smaller size and disorganization of the mutant embryo (×100). The bracket delineates the extraembryonic region. ep, ectoplacental cavity; ex, exoceolom; am, amniotic cavity; rm, Reichert's membrane. (*C* and *D*) Morphologic demonstration of embryonic ectoderm (ec), mesoderm (m), and endoderm (en) in H & E stained paraffin sections of wild-type and mutant embryos (×250). (*E* and *F*) *In situ* hybridization using a *Brachyury* (T gene) probe. T gene hybridization signal (arrow head) was detected in both wild-type and mutant embryos (×100). (*G* and *H*) *In situ* hybridization using *Cerr1* probe. *Cerr1* hybridization signal (arrow head) was detected in anterior endoderm of both wild-type and mutant embryos (×100). (*I* and *J*) Immunodectection of PCNA. A similar level of expression (dark brown stain) is seen in the wild-type and mutant embryo. Arrows point out some examples of positive cells (×250). (*K* and *L*) TUNEL detection of apoptotic cells. Greatly enhanced incidence of TUNEL-positive nuclei (small, dark brown spots) was seen in the mutant embryo, especially in the ectodermal layer. Arrows point to some of the many positive reactions in the mutant embryo. Only a few positive reactions were found in the wild-type embryo (×250).

wild-type tumors by morphologic criteria (Fig. 4 *H* and *I*) but were totally absent from the mutant tumors. Although mesodermally derived tissue was present in the mutant tumors, as determined by vimentin immunostaining, it was not of any distinctive morphology. Mature, well differentiated epithelial tissues—bronchial with associated glands, colonic, and squamus—were also abundant in the wild-type tumors (Fig. 4*F*). These well differentiated epithelial tissues were largely absent from the mutant tumors; only a very minor component of bronchial epithelial tissue was noted (Fig. 4*G*). Both wild-type and mutant tumors were generally similar in the expression of PCNA antigen and in the incidence of apoptotic cells (data not shown).

DISCUSSION

Our results indicate that GSL synthesis is critical for embryonic development and for differentiation of certain tissues. Earlier studies have suggested an important role for cell-surface carbohydrate interactions in preimplantation embryogenesis, although the nature of these structures, whether glycolipid or glycoprotein, could not be ascertained. The Le^X structure, found on both glycoproteins and GSLs, was shown to be important for embryo compaction at the morula stage (36). Elimination of *O*-acetylated sialic acids, found on some gangliosides in addition to glycoproteins, aborted development at the two-cell stage (37). Our results indicate that embryos defective in GSL synthesis are able to proceed through preimplantation development. We cannot rule out, however, the possibility that maternally derived *Ugcg* mRNA or that residual GSLs may suffice for these very early stages of embryogenesis. It also is not known whether galactose-based GSLs (Fig. 1*A*) are expressed at this stage and whether they might substitute for the absence of the glucose-based GSLs.

The homozygous $Ugcg^{\Delta EX7Neo}$ embryos underwent implantation into the uterus and appeared normal at the egg cylinder stage. Implicit in the attainment of this developmental stage is a functional interaction between embryo and uterus giving rise to a decidual reaction. Gastrulation initiated in the mutant embryos with clear differentiation into embryonic germ layers, mesoderm, endoderm, and ectoderm as well as the regional expression of certain critical genes, indicating proper patterning of the embryo. However, the gastrulating embryo died abruptly and was reabsorbed. Embryonic death was most probably caused by massive apoptosis largely, but not exclusively, focused in the ectodermal layer.

A primary defect in ectoderm could have led to apoptosis in the *Ugcg* mutant embryos and may reflect the fact that this lineage is a precursor to the developing nervous system, where gangliosides are abundantly expressed. If GSLs are essential for neuronal differentiation, then their function may only be vital in the context of the developing embryo because the mutant ES cells without glucosylceramide synthase retained the capacity to undergo neuronal differentiation in culture via induction with retinoic acid.

The expression of the *Ugcg* gene was found throughout the gastrulating embryo (T.Y. and R.L.P., unpublished work), raising the possibility that the ectodermal apoptosis might be attributable to abnormalities in other elements of the embryo. In both E7.5 *HNF-4* (38) and huntingtin (*Hdh*) (39) knock-out embryos, a very similar ectodermal apoptotic pattern was observed that was later attributed to primary defects in visceral endoderm (40, 41). However, no apparent defects in visceral endoderm could be detected in the *Ugcg* mutant embryos, as determined morphologically or by the expression of the lineage-specific transcription factor, *HNF3β*.

Ceramide has been reported to be an apoptotic trigger in some circumstances (42, 43), and its accumulation as a result of the

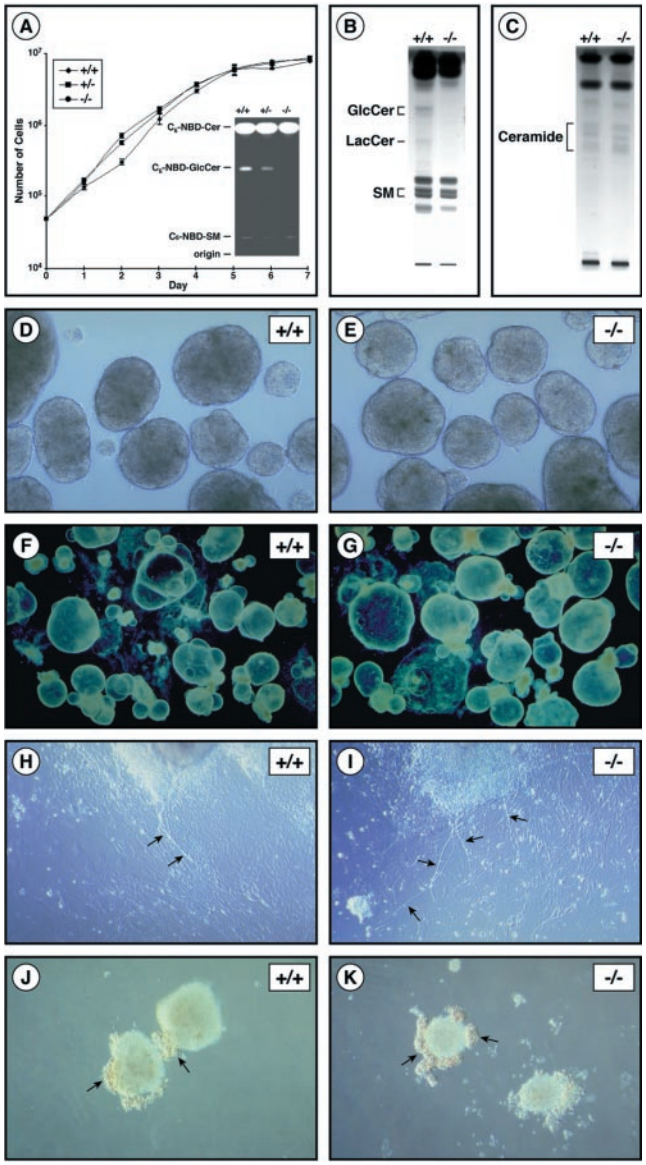

FIG. 3. *In vitro* growth and differentiation of ES cells in the absence of GSL synthesis. (*A Left*) Growth of wild-type (+/+), $Ugcg^{\Delta EX7Neo/+}$ (+/−), and $Ugcg^{\Delta EX7Neo/\Delta EX7Hygro}$ (−/−) ES cells. ES cells (5×10^4) were seeded into 60-mm plates containing mitomycin C-treated embryonic fibroblasts to initiate the experiment. Each day the medium was changed and the cells from one plate were harvested and were counted. (*Inset*) Glucosylceramide synthase activity in wild-type (+/+), $Ugcg^{\Delta EX7Neo/+}$ (+/−), and $Ugcg^{\Delta EX7Neo/\Delta EX7Hygro}$ (−/−) ES cells. Each cell extract, corresponding to 50 μg of protein, was incubated with C6-NBD-ceramide and UDP-glucose. After incubation, lipids were separated by high-performance thin-layer chromatography (HPTLC) and were visualized by UV illumination. The positions of the C6-NBD derivatives of glucosylceramide (C6-NBD-GlcCer) lactosylceramide (C6-NBD-LacCer) and sphingomyelin (C6-NBD-SM) are indicated (*B*) HPTLC analysis of neutral glycolipids isolated from wild-type (+/+) and $Ugcg^{\Delta EX7Neo/\Delta EX7Hygro}$ (−/−) ES cells. The positions of glucosylceramide (GlcCer), lactosylceramide (LacCer), and sphingomyelin (SM) are indicated. (*C*) HPTLC analysis of ceramide levels in wild-type (+/+) and $Ugcg^{\Delta EX7Neo/\Delta EX7Hygro}$ (−/−) ES cells. The position of ceramide is indicated. (*D* and *E*) Wild-type (+/+) and $Ugcg^{\Delta EX7Neo/\Delta EX7Hygro}$ (−/−) embryoid bodies after 3 days of culture (×60). (*F* and *G*) Wild-type (+/+) and $Ugcg^{\Delta EX7Neo/\Delta EX7Hygro}$ (−/−) cystic embryoid bodies after 22 days of culture (×20). (*H* and *I*) Retinoic acid-induced neuronal differentiation of wild-type (+/+) and $Ugcg^{\Delta EX7Neo/\Delta EX7Hygro}$ (−/−) ES cells (×100). Arrows indicate neurite formation. (*J* and *K*) Erythropoietin-induced hematopoietic differentiation of wild-type (+/+) and $Ugcg^{\Delta EX7Neo/\Delta EX7Hygro}$ (−/−) ES cells (×100). Arrows indicate clusters of red erythroid cells surrounding embryoid bodies.

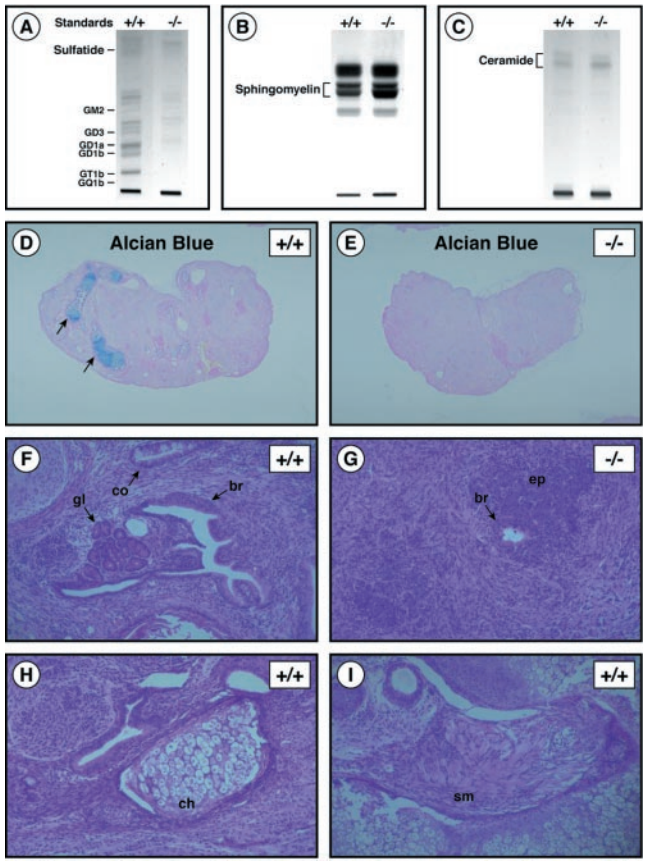

FIG. 4. *In vivo* differentiation of teratomas in the absence of GSL synthesis. (*A*) Acidic lipid fractions from of wild-type (+/+) and $Ugcg^{\Delta EX7Neo/\Delta EX7Hygro}$ (−/−) teratomas analyzed by HPTLC. The position of GSL standards are indicated on the left. (*B*) HPTLC analysis of sphingomyelin levels from of wild-type (+/+) and $Ugcg^{\Delta EX7Neo/\Delta EX7Hygro}$ (−/−) teratomas. The position of sphingomyelin is indicated. (*C*) HPTLC analysis of ceramide levels in wild-type (+/+) and $Ugcg^{\Delta EX7Neo/\Delta EX7Hygro}$ (−/−) teratomas. The position of ceramide is indicated. (*D* and *E*) Sections of wild-type (+/+) and $Ugcg^{\Delta EX7Neo/\Delta EX7Hygro}$ (−/−) teratomas stained with Alcian blue (×5). Arrows indicate Alcian blue-positive cartilage in the wild-type tumor but not found in the mutant tumor. (*F*) H & E-stained section of the wild-type teratoma showing well differentiated epithelial tissues (×100). gl, glands; br, bronchial epithelium; co, colonic epithelium. (*G*) H & E-stained section of $Ugcg^{\Delta EX7Neo/\Delta EX7Hydro}$ (−/−) teratoma showing poorly differentiated epithelial tissue (ep) and small focus of bronchial epithelium (br) (×100). (*H*) H & E-stained section of a wild-type teratoma showing chondrocytes (ch) (×100). (*I*) H & E-stained section of the wild-type teratoma showing smooth muscle (sm) (×100).

deficiency in glucosylceramide synthase also must be considered a potential cause of embryonic apoptosis and death. The small size of the embryos precluded a direct determination of their ceramide levels. Neither elevated ceramide levels nor increased apoptosis were found in mutant ES cells, indicating that the absence of glucosylceramide synthase does not inevitably lead to ceramide accumulation and cell death.

GSLs are believed to influence cellular proliferation. Possible mechanisms include GSL modulation of signaling by interactions with tyrosine kinases associated with growth-factor receptors (4) and through the elaboration of GSL metabolites that have potent effects on cell growth (44). We did not find evidence of growth defects caused by the absence of GSL synthesis in embryos up to E6.5, tumors, or cultured cells. It is possible, however, that primitive cells types may not use these mechanisms.

Differentiation defects caused by the absence of GSL synthesis were observed in the mutant teratomas. Without GSL synthesis, the mutant tumors consisted primarily of poorly differentiated

tissues. Like the homozygous *Ugcg*$^{\Delta EX7Neo}$ embryos, the mutant tumors contained immature tissues derived from the three primitive germ layers. These tissues were identified as neuroepithelium (ectoderm), mesenchymal cells (mesoderm), and bronchial epithelium (endoderm). A striking finding was the near absence of well differentiated tissues in the mutant tumors. By contrast, the wild-type tumors contained mature tissues such as smooth muscle, cartilage, and well differentiated epithelia. Other studies also have indicated that GSLs may be essential for differentiation of tissues. Transgenic mice with selective expression of sialic acid-specific 9-*O*-acetylesterase showed morphologic abnormalities in retina and adrenal gland together with the absence of 9-*O*-acetyl-G_{D3} ganglioside (37). Antibody to G_{D3} ganglioside interfered with inductive epithelial–mesenchymal interactions and epithelial morphogenesis (45). With the cultured epithelial line, MDCK cells, it was shown that antibody to the Forssman glycolipid—a GSL—inhibited adhesion of the cells to laminin and blocked the process of epithelial polarization (46). The absence of GSLs in the mutant tumors may have precluded critical cell-to-cell and cell-to-matrix interactions, resulting in impaired formation of well differentiated tissues. We found that the undifferentiated mutant ES cells were equal to wild-type cells in their ability to adhere to matrix proteins (fibronectin, laminin, and collagen) and to glycolipids (lactosylceramide, GM3, and asialoGM2) in a solid phase assay (R.W. and R.L.P., unpublished work). If GSLs are involved in adhesion, then they may not manifest this function in primitive cells.

Such profound differentiation defects were not observed, however, *in vitro.* Mutant ES cells, without the capacity to synthesize GSLs, proceeded from embryoid bodies to a cavitated cystic body structure. These steps required the formation of endodermal and ectodermal cells and the creation of a central cavity mediated by a controlled apoptotic process (34). This limited *in vitro* differentiation recapitulates aspects of preimplantation development and differentiation and is, therefore, consistent with the normal preimplantation development of homozygous Ugcg$^{\Delta EX7Neo}$ embryos. ES cells, despite the absence of GSL synthesis, also retained the capacity, under the stimulation of retinoic acid and erythropoietin, to differentiate into ectoderm-derived neuronal cells and to mesoderm-derived erythroid cells.

Collectively, the results indicate that, in the absence of GSL synthesis, differentiation of pluripotent cells can proceed at least into primitive cell lineages. In mutant embryos and teratomas, further differentiation was clearly impaired without GSL synthesis. During gastrulation, precise spatiotemporal coordination of cell behaviors—signaling, cell interactions, and migration—is critical for subsequent morphogenesis (47). A participation of GSLs in these functions would be entirely consistent with the observed lethality of the mutant embryos. An inability to correctly integrate extracellular signals may have resulted in apoptosis and embryonic death (48). Likewise, in the milieu of the teratoma, inductive cell interactions—cell-to-cell and cell-to-matrix—may be impaired by the absence of GSLs, blocking the formation of mature, well differentiated tissues. Neuronal and erythroid differentiation *in vitro*, which were induced by exogenous stimuli, proceeded in the absence of GSL synthesis and may be a reflection that differentiation in the simpler culture system is less dependent on critical cell interactions than is differentiation in the context of the embryo and teratoma. Disruption of other glycosyltransferases to yield small, defined GSL structures will be a necessary next step for understanding the precise roles of GSLs in development and differentiation.

We thank Mike Weinstein for comments on the manuscript, Cuiling Li for excellent technical assistance, and Jenn Reed for her expert help in preparing the figures. We thank Richard Behringer and William Shawlot for the *Cerr1* probe. This work was supported in part by a grant from the Deutsche Forschungsgemeinschaft (SFB 284) to K.S.

1. Svennerholm, L. (1994) *Prog. Brain Res.* **101,** x–xiv.
2. Kolter, T. & Sandhoff, K. (1998) *Brain Pathol.* **8,** 79–100.
3. Hakomori, S. (1990) *J. Biol. Chem.* **265,** 18713–18716.
4. Hakomori, S. & Igarashi, Y. (1995) *J. Biochem. (Tokyo)* **118,** 1091–1103.
5. Nagai, Y. & Tsuji, S. (1994) *Prog. Brain Res.* **101,** 119–126.
6. Ichikawa, S. & Hirabayashi, Y. (1998) *Trends Cell Biol.* **8,** 198–202.
7. van Meer, G. (1998) *Trends Cell Biol.* **8,** 29–33.
8. Varki, A. (1993) *Glycobiology* **3,** 97–130.
9. Schnaar, R. L. (1991) *Glycobiology* **1,** 477–485.
10. Tettamanti, G. & Riboni, L. (1993) *Adv. Lipid Res.* **25,** 235–267.
11. Simons, K. & Ikonen, E. (1997) *Nature (London)* **387,** 569–572.
12. Harder, T. & Simons, K. (1997) *Curr. Opin. Cell Biol.* **9,** 534–542.
13. Anderson, R. G. (1998) *Annu. Rev. Biochem.* **67,** 199–225.
14. Huang, C., Hepler, J. R., Chen, L. T., Gilman, A. G., Anderson, R. G. W. & Mumby, S. M. (1997) *Mol. Biol. Cell* **8,** 2365–2378.
15. Hakomori, S., Handa, K., Iwabuchi, K., Yamamura, S. & Prinetti, A. (1998) *Glycobiology* **8,** xi–xix.
16. Iwabuchi, K., Handa, K. & Hakomori, S. (1998) *J. Biol. Chem.* **273,** 33766–33773.
17. Jeckel, D., Karrenbauer, A., Burger, K. N., van Meer, G. & Wieland, F. (1992) *J. Cell Biol.* **117,** 259–267.
18. Futerman, A. H. & Pagano, R. E. (1991) *Biochem. J.* **280,** 295–302.
19. Marks, D. L., Wu, K., Paul, P., Kamisaka, Y., Watanabe, R. & Pagano, R. E. (1999) *J. Biol. Chem.* **274,** 451–456.
20. Capecchi, M. R. (1989) *Science* **244,** 1288–1292.
21. van Deursen, J. & Wieringa, B. (1992) *Nucleic Acids Res.* **20,** 3815–3820.
22. Deng, C., Wynshaw-Boris, A., Zhou, F., Kuo, A. & Leder, P. (1996) *Cell* **84,** 911–921.
23. Liu, Y., Wada, R., Kawai, H., Sango, K., Deng, C., Tai, T., McDonald, M. P., Araujo, K., Crawley, J. N., Bierfreund, U., *et al.* (1999) *J. Clin. Invest.* **103,** 497–505.
24. Kawai, H., Sango, K., Mullin, K. A. & Proia, R. L. (1998) *J. Biol. Chem.* **273,** 19634–19638.
25. Deng, C. X., Wynshaw-Boris, A., Shen, M. M., Daugherty, C., Ornitz, D. M. & Leder, P. (1994) *Genes Dev.* **8,** 3045–3057.
26. Shawlot, W., Deng, J. M. & Behringer, R. R. (1998) *Proc. Natl. Acad. Sci. USA* **95,** 6198–6203.
27. Dufort, D., Schwartz, L., Harpal, K. & Rossant, J. (1998) *Development (Cambridge, U.K.)* **125,** 3015–3025.
28. Ang, S. L., Conlon, R. A., Jin, O. & Rossant, J. (1994) *Development (Cambridge, U.K.)* **120,** 2979–2989.
29. Poirier, F., Chan, C. T., Timmons, P. M., Robertson, E. J., Evans, M. J. & Rigby, P. W. (1991) *Development (Cambridge, U.K.)* **113,** 1105–1114.
30. Kon, Y., Endoh, D., Fukamizu, A., Murakami, K., Yamashita, T. & Watanabe, T. (1996) *Anat. Histol. Embryol.* **25,** 289–294.
31. Lipsky, N. G. & Pagano, R. E. (1985) *Science* **228,** 745–747.
32. Robertson, E. J. (1987) in *Teratocarcinomas and Embryonic Stem Cells*, ed. Robertson, E. J. (IRL, Oxford).
33. DiCristofano, A., Pesce, B., Cordon-Cardo, C. & Pandolfi, P. P. (1998) *Nat. Genet.* **19,** 348–355.
34. Coucouvanis, E. & Martin, G. R. (1995) *Cell* **83,** 279–287.
35. Bain, G., Kitchens, D., Yao, M., Huettner, J. E. & Gottlieb, D. I. (1995) *Dev. Biol.* **168,** 342–357.
36. Eggens, I., Fenderson, B., Toyokuni, T., Dean, B., Stroud, M. & Hakomori, S. (1989) *J. Biol. Chem.* **264,** 9476–9484.
37. Varki, A., Hooshmand, F., Diaz, S., Varki, N. M. & Hedrick, S. M. (1991) *Cell* **65,** 65–74.
38. Chen, W. S., Manova, K., Weinstein, D. C., Duncan, S. A., Plump, A. S., Prezioso, V. R., Bachvarova, R. F. & Darnell, J. E., Jr. (1994) *Genes Dev.* **8,** 2466–2477.
39. Zeitlin, S., Liu, J. P., Chapman, D. L., Papaioannou, V. E. & Efstratiadis, A. (1995) *Nat. Genet.* **11,** 155–163.
40. Duncan, S. A., Nagy, A. & Chan, W. (1997) *Development (Cambridge, U.K.)* **124,** 279–287.
41. Dragatsis, I., Efstratiadis, A. & Zeitlin, A. (1998) *Development (Cambridge, U.K.)* **125,** 1529–1539.
42. Kolesnick, R. N. & Kronke, M. (1998) *Annu. Rev. Physiol.* **60,** 643–665.
43. Hannun, Y. A. & Obeid, L. M. (1997) *Biochem. Soc. Trans.* **25,** 1171–1175.
44. Spiegel, S. & Merrill, A. H., Jr. (1996) *FASEB J.* **10,** 1388–1397.
45. Sariola, H., Aufderheide, E., Bernhard, H., Henke-Fahle, S., Dippold, W. & Ekblom, P. (1988) *Cell* **54,** 235–245.
46. Zinkl, G. M., Zuk, A., van der Bijl, P., van Meer, G. & Matlin, K. S. (1996) *J. Cell Biol.* **133,** 695–708.
47. Tam, P. P. & Behringer, R. R. (1997) *Mech. Dev.* **68,** 3–25.
48. Jacobson, M. D., Weil, M. & Raff, M. C. (1997) *Cell* **88,** 347–354.